Applied Catalysis B: Environmental 224 (2018) 572–578

Contents lists available at ScienceDirect

Applied Catalysis B: Environmental

journal homepage: www.elsevier.com/locate/apcatb

Research Paper

Enhancement of CO_2 reduction activity under visible light irradiation over Zn-based metal sulfides by combination with Ru-complex catalysts

Tomiko M. Suzuki[a,*], Tomoaki Takayama[b], Shunsuke Sato[a], Akihide Iwase[b], Akihiko Kudo[b], Takeshi Morikawa[a,*]

[a] Toyota Central R & D Labs. Inc., 41-1, Yokomichi, Nagakute, Aichi 480-1192, Japan
[b] Tokyo University of Science, Department of Applied Chemistry, 1-3 Kagurazaka, Shinjuku-ku, Tokyo 162-8601, Japan

ARTICLE INFO

Keywords:
CO_2 reduction
Metal-complex
Metal sulfide
Photocatalyst
Visible-light

ABSTRACT

Hybrid photocatalysts composed of metal sulfide semiconductors combined with various Ru-complex catalysts were synthesized for use during visible light-driven CO_2 reduction with powder suspension systems. A variety of Zn-based sulfides, including Ni-doped ZnS, $(CuGa)_{0.8}Zn_{0.4}S_2$ and $(AgIn)_{0.22}Zn_{1.56}S_2$, were adopted by conducting the CO_2 reduction reaction in acetonitrile containing an electron donor. The photocatalytic activities were found to be largely dependent on the basic characteristics of the Ru-complex and the metal sulfide. The results demonstrate that several of these sulfide semiconductors improve the CO_2 reduction selectivity when employed in the semiconductor/metal-complex system, and that $(AgIn)_{0.22}Zn_{1.56}S_2$ or Ni (0.2 mol%)-doped ZnS combined with a neutral Ru-complex incorporating a phosphonate ligand [Ru(4,4′-diphosphonate-2,2′-bipyridine)$(CO)_2Cl_2$] exhibit the highest CO_2 photoconversion activity when synthesizing formic acid, with a turnover number above 100, which catalysts were stable for 16 h irradiation. These results suggest that metal sulfides are potential candidates for use in powdered semiconductor/metal-complex systems for selective CO_2 photoreduction.

1. Introduction

The reduction of CO_2 to obtain useful energy-rich chemicals utilizing photocatalysts in water has attracted attention as a potential means of artificial photosynthesis operating under solar irradiation. As such, there have been many studies regarding photoelectrochemical systems incorporating photoelectrodes for both generation of H_2 [1] and organic substances [2], although relatively few assessments of powdered photocatalytic systems. These powdered photocatalysts are attractive as potential devices for the practical, cost-effective generation of H_2 by water splitting [3]. In contrast, the use of powdered systems for CO_2 reduction is challenging owing to the inherent difficulty in achieving the selective reaction of CO_2 in solution and obtaining efficient photoexcited electron transfer from the oxidation sites to the CO_2 reduction sites in a heterogeneous environment. The combination of a semiconductor photosensitizer and a metal complex catalyst is one promising approach to selective CO_2 reduction under visible light irradiation. A hybrid composed of *p*-type N-doped Ta_2O_5 (N-Ta_2O_5) [4] with $[Ru(dcbpy)_2(CO)_2]^{2+}$ (dcbpy: 4,4′-dicarboxy-2,2′-bipyridine, hereafter [Ru(dcbpy)$_2$]) suspended in acetonitrile (MeCN) has been shown to catalyze visible light-induced CO_2 reduction to formate using triethanolamine (TEOA) as an electron donor and proton source. This process is based on the efficient coordination of CO_2 molecules with the Ru-complex [5,6]. Interestingly, although N-Ta_2O_5 or [Ru(dcbpy)$_2$] alone do not photocatalyze CO_2 reduction under visible irradiation, the CO_2 reduction reaction proceeds over a [Ru(dcbpy)$_2$]/N-Ta_2O_5 hybrid. Experimental and theoretical investigations have suggested that the energy difference, ΔG, between the conduction band minimum (E_{CBM}) of N-Ta_2O_5 and the LUMO of the Ru-complex is a very important factor that facilitates electron transfer from N-Ta_2O_5 in the photoexcited state to the Ru-complex [5–9], with the time constant of the electron transfer on the order of tens of picoseconds [10]. Ishitani and Maeda's group has reported powdered photocatalysts composed of a visible light-sensitive *n*-type oxynitride semiconductor (TaON) combined with Ru–Ru binuclear complex photocatalysts in MeOH [11] or aqueous solutions containing ethylenediaminetetraacetic acid disodium salt (EDTA) as an electron donor [12]. This same group has also demonstrated a carbon nitride (C_3N_4) semiconductor combined with Ru-complexes in various organic solvents (such as *N*, *N*-dimethylacetamide, MeCN, and MeOH/TEOA) [13,14] or aqueous solutions containing an electron donor [14], with the generation of formic acid from CO_2. Cowan and Durrant group demonstrated photocatalytic CO_2

* Corresponding authors.
E-mail addresses: tomiko@mosk.tytlabs.co.jp (T.M. Suzuki), morikawa@mosk.tytlabs.co.jp (T. Morikawa).

http://dx.doi.org/10.1016/j.apcatb.2017.10.053
Received 20 August 2017; Received in revised form 21 October 2017; Accepted 24 October 2017
Available online 07 November 2017
0926-3373/

reduction in protic solvents using nickel cyclam catalysts immobilized on semiconductor materials including TiO_2 and $Ti_{1-x}Zr_xO_2$ [15].

Metal sulfide semiconductors, known to function as highly efficient visible light-driven hydrogen evolution photocatalysts in aqueous solutions in the presence of sacrificial hole scavengers, are also attractive for CO_2 photocatalysis. Metal sulfides generally have narrower band gaps than metal oxides due to the shallower valence bands formed by S 3p orbitals compared to those formed by O 2p orbitals [16]. Among the metal sulfides, both undoped CdS (with a band gap of 2.4 eV) [17–19] and ZnS (3.5 eV) [20] have been studied. ZnS in particular is recognized as an attractive host material for impurity doping and the formation of solid solutions for water splitting reactions. Because of its wide band gap, ZnS exhibits photoactivity only under UV irradiation [16,20], although doping with metal cations (Ni^{2+} [21], Cu^{2+} [22] or Pb^{2+} [23]) leads to efficient H_2 evolution activity in the presence of the electron donor species SO_3^{2-} under visible light irradiation, even without a metal cocatalyst. Doping with metals produces a new energy level in the band gap of ZnS due to the Ni 3d, Cu 3d, or Pb 3d orbitals. In addition, solid solutions based on ZnS such as $(CuGa)_{1-x}Zn_{2x}S_2$ [24], $(AgIn)_xZn_{2(1-x)}S_2$ [25–27] and $(CuIn)_xZn_{2(1-x)}S_2$ [27,28] can be formed by adding the narrow band gap semiconductors CuGaS, $AgInS_2$ and $CuInS_2$. These materials are attractive because the band position of the solid solution can be tuned by changing the semiconductor. The conduction and valence bands of $(CuGa)_{1-x}Zn_{2x}S_2$ primarily consist of Zn 4s4p + Ga 4s4p and Cu 3d + S 3p orbital combinations, respectively. The Zn 4s4p orbitals form a conduction band at a higher (more negative) level than the Ga 4s4p orbitals [24]. This orbital hybridization induces a redshift in the photo-response of the materials, such that photocatalytic hydrogen evolution has been demonstrated in aqueous sulfide and sulfite solutions containing the electron donor SO_3^{2-} at longer wavelengths than ZnS by Kudo's group [24–28]. Recently, CO_2 reduction using $CuGaS_2$ and Ni-doped ZnS in aqueous solution has also been reported [29]. In this work, HCOOH and CO were generated from CO_2 in aqueous solution in the presence of the electron donors K_2SO_3 and Na_2S without the loading of co-catalysts.

Based on the above, sulfide semiconductors are a strong candidate for use in complex/semiconductor hybrid systems having higher CO_2 reduction selectivity. Recently, Reisner et al. reported a photocatalytic CO_2 reduction system of a molecular Ni catalyst linked with CdS nanocrystals with CO selectivity of > 90% [30]. Among these, Zn-based sulfides are considered to be superior because ZnS possesses a relatively negative E_{CBM} as a result of the Zn 4s4p orbitals, which facilitates the electron transfer from the conduction band of the semiconductor in a photoexcited state to the metal complex catalyst. Cu_2ZnSnS_4 (CZTS) has been examined as a photocathode for CO_2 reduction by our own group, modified with polymerized [Ru{4,4′-di(1*H*-pyrrolyl-3-propylcarbonate)-2,2′-bipyridine}(CO)(MeCN)Cl_2] (hereafter [Ru(pypcbpy)]) [31]. Useable powdered hybrid systems have not yet been reported. Interestingly, powdered ZnS:Ni (0.1 mol% Ni) with [Ru(4,4′-dicarboxy-2,2′-bipyridine)(2,2′-bipyridine)$(CO)_2]^{2+}$ did not promote the photocatalytic CO_2 reduction reaction in a MeCN/TEOA solution, even though the ΔG driving the electron transfer should have been sufficient [5].

In the present study, the powdered Ni-doped ZnS semiconductors $(CuGa)_{0.8}Zn_{0.4}S_2$, and $(AgIn)_{0.22}Zn_{1.56}S_2$, which are active for sacrificial H_2 evolution, were investigated in combination with various Ru-complex catalysts with regard to the promotion of visible light induced CO_2 reduction. Working in MeCN/TEOA solutions, the effects of the anchoring groups and the charge of the Ru-complexes on photocatalytic CO_2 reduction were investigated using these ZnS:Ni materials. The results indicate that Zn-based sulfide semiconductors having various bandgaps and band positions are readily applicable as hybrid photocatalysts for CO_2 reduction under visible light irradiation.

2. Experimental

2.1. Preparation of the metal sulfide semiconductor

Ni-doped ZnS (0.2 mol% Ni) [21] was prepared by mixing an aqueous solution of $Zn(NO_3)_2$ and $Ni(NO_3)_2$ with an aqueous solution of Na_2S at room temperature. The resulting precipitate was washed with distilled water, filtered and dried in air, then heated at 773 K for 2 h under an Ar flow. Non-doped ZnS was also prepared using an aqueous $Zn(NO_3)_2$ solution and employing the same method. $(CuGa)_{0.8}Zn_{0.4}S_2$ [24] and $(AgIn)_{0.22}Zn_{1.56}S_2$ [25,26] were prepared according to previously reported procedures.

2.2. Synthesis of the Ru-complex

[Ru(4,4′-dicarboxy-2,2′-bipyridine)$_2$(CO)$_2$]$^{2+}$ ([Ru(dcbpy)$_2$]) [5], (4,4′-diphosphonate-2,2′- bipyridine)(CO)$_2$]$^{2+}$ ([Ru(dpbpy)-(bpy)]) [6], [Ru (4,4′-diphosphonate-2,2′-bipyridine)(CO)$_2$Cl ([Ru(dpbpy)]) [32], [Ru (4,4′-dicarboxy-2,2′-bipyridine)(CO)$_2$Cl ([Ru(dcbpy)]) [32], [Ru(2,2′-bipyridine)] and [Ru{4,4′-di(1H-pyrrolyl-3-propyl carbonate)-2,2′- bipyridine}(CO)(MeCN)Cl$_2$] ([Ru(pypcbpy)]) [33] were synthesized according to previously reported methods.

2.3. Preparation of the Ru-complex/metal sulfide hybrid photocatalysts (adsorption method)

Hybrid photocatalysts consisting of a Ru-complex ([Ru(dcbpy)$_2$], [Ru(dpbpy)(bpy)], [Ru(dpbpy)], or [Ru(dcbpy)]) and a metal sulfide were prepared by adsorption of the Ru-complex. A mixture of the metal sulfide powder (200 mg) and a solution of the Ru-complex (0.4 mg) in methanol (5 mL) was stirred overnight under dark conditions. The solution was subsequently filtered, washed with methanol and dried under vacuum at 313 K. The absorption spectra of these solutions after filtration were acquired using a UV/vis spectrophotometer (Shimadzu, UV-3600) and the amount of Ru-complex adsorbed on the metal sulfide was calculated from each spectrum.

2.4. Preparation of the [Ru(pypcbpy)]/ZnS:Ni hybrid photocatalyst (photopolymerization method)

A hybrid photocatalyst consisting of [Ru(pypcbpy)] and ZnS:Ni was prepared by photopolymerization of the Ru-complex. A mixture of ZnS:Ni powder and [Ru(pypcbpy)] (0.4 mg) in acetonitrile (5 mL) was stirred overnight under fluorescent lamp irradiation. The post-processing method was the same as that described above for the adsorption method.

2.5. Characterization

The crystal structures of the samples were assessed using X-ray diffraction (XRD, Rigaku, Ultima IV) with Cu Kα radiation at 40 kV and 40 mA. Surface areas were determined by BET measurement (Coulter, SA3100). The chemical structures of the hybrid photocatalysts were characterized using diffuse reflectance infrared Fourier transform spectroscopy (DRIFTS; JASCO, JNM-LA500). Diffuse reflection spectra were obtained using a UV–vis-NIR spectrometer (JASCO, V-780) and were converted from reflectance to absorbance by the Kubelka–Munk method. X-ray photoelectron spectroscopy (XPS; Ulvac-Phi Quantera SXM) was also conducted, with monochromated Al Kα radiation.

2.6. Photocatalytic reaction for CO_2 reduction in MeCN/TEOA

The photocatalytic activity of each hybrid photocatalyst was measured under ambient pressure in an 8 mL test tube containing 4 mL of a dry acetonitrile (MeCN)-triethanolamine (TEOA) mixture (5:1 by volume) and 8 mg of the photocatalyst. After purging with CO_2 for

15 min, the suspension was irradiated in a rotating apparatus using a 500 W Xe lamp (Ushio UXL-500SX), equipped with filters to produce visible light in the range of 390 $< \lambda \leq$ 750 nm at 31 mW/cm^2 for 16 h at room temperature, in the same manner as reported in a previous study [6]. The amount of product obtained was determined by gas chromatography (Shimadzu, GC-14A) and ion exchange chromatography (Dionex, ICS-2000).

2.7. Isotope analysis

To detect the formation of $H^{13}COOH$, an ion chromatograph interfaced with a time-of-flight mass spectrometer (IC-TOFMS, JEOL JMS-T100LP) was used, with MeOH as the mobile phase.

3. Results and discussion

3.1. Synthesis of various Ru-complex/ZnS:Ni hybrid photocatalysts and CO_2 photoreduction

To investigate the feasibility of using metal sulfide semiconductors in hybrid photocatalysts, the visible light photoactive *n*-type material Ni (0.2 mol%)-doped ZnS [ZnS:Ni (0.2%)] [21], with an energy gap of 2.3 eV, was selected. The crystalline structure and morphology of the ZnS:Ni were confirmed by X-ray diffraction (XRD) and field emission-scanning electron microscopy (FE-SEM). The material was found to consist of a mixture of zinc-blende and a small amount of wurtzite, with cubic particles having diameters in the range of 30–100 nm (Figs. S1 and S2). The BET surface area of the material was also estimated to be 6.4 m^2/g. Although the energy level of the conduction band minimum of this semiconductor ($E_{CBM} = -1.3$ V *vs.* NHE), composed of Zn 4s4p orbitals [16], is sufficient to promote the transfer of electrons from the conduction band to the Ru-complex catalyst, CO_2 photoreduction did not proceed in MeCN/TEOA solutions in a previous study using [Ru(dcbpy)$_2$]/ZnS:Ni [4]. In the present work, ZnS:Ni in powder form was synthesized according to the solution method reported by Kudo et al. [21].

The optimal combination of ZnS:Ni and a Ru-complex was ascertained by investigating five different Ru-complex catalysts with various anchors (phosphonate or carboxylate), charges (neutral or cationic), and CO_2 reduction potentials (-1.0 to -0.6 V *vs.* NHE, [5]) (Fig. 1 and Table 1). The potentials of catalytic CO_2 reduction were measured by cyclic voltammograms in MeCN purged with CO_2. All these factors are known to affect the efficiency of electron transfer during the CO_2 reduction reaction over the complexes.

The chemical structures of the hybrid catalysts prepared by adsorption of Ru-complex onto ZnS:Ni were characterized using DRIFTS and successful modification of Ru-complex were confirmed (Fig. S3). The amounts of loaded Ru-complex catalysts on ZnS:Ni were also calculated to be 0.05–0.07 wt% as shown in Table 2. The UV–vis diffuse reflectance spectra of before and after modification of Ru-complex onto the semiconductor were almost same, because the absorption peaks of Ru-complex were completely overlapped with ZnS:Ni due to low amount of the Ru-complex (Fig. S4). These results indicate that ZnS:Ni plays a significant role as the light absorber of these hybrid photocatalysts.

CO_2 photoreduction over each ZnS:Ni/Ru-complex hybrid photocatalyst was performed in a MeCN solution containing TEOA as an electron donor under visible light irradiation ($\lambda > 390$ nm) for 16 h, similar to the approach used with previous N-Ta_2O_5 and C_3N_4 and other powdered systems [5–7,13,14,30,34]. It was reported that solubility of CO_2 in MeCN was more than eight times higher than that in aqueous solution [35], and it is considered to be effective solvent for CO_2 reduction. To clarify the effect of the modification of Ru-complex, the Ru-complex catalyst turnover number (TON) was calculated on the basis of the product produced by Ru-complex (deducted from the amount of the product produced by the originated semiconductor). As shown in Table 2, unmodified ZnS:Ni was found to promote H_2 evolution by proton reduction but not CO_2 photoreduction (entry 1). In this case, the proton source for the synthesis of H_2 is believed to have been the TEOA, judging from previous results reported in the literature [5]. In addition, the Ru-complex alone did not show photocatalytic activity (entry 2). The use of a cationic Ru-complex with carboxylate groups ([Ru(dcbpy)$_2$]), which has been reported to be highly effective in conjunction with N-Ta_2O_5 [5], generated very little photocatalytic CO_2 reduction but produced more H_2 than unmodified N-Ta_2O_5 (entry 3), which was consistent with the previous study [36]. A Ru-complex with a similar structure, [Ru(4,4′-dicarboxy-2,2′-bipyridine)-(2,2′-bipyridine)(CO)$_2$]$^{2+}$, did not yield CO_2 reduction products, in keeping with previously reported results [5]. These data indicate that the combination of cationic Ru-complexes having carboxylate anchors with ZnS:Ni does not photoreduce CO_2. The CO_2 reduction potential at the Ru-complex is important because the activity is determined by the extent to which the Ru-complex receives electrons from the photoexcited semiconductor in the semiconductor/metal-complex hybrid [5,6,9,10]. Interestingly, even though the CO_2 reduction potential (-0.8 V *vs.* NHE) was unchanged from that of [Ru(dcbpy)$_2$] (Table 1), the substitution of a phosphonate anchor for a carboxylate group on one of the bipyridine ligands (that is, the use of [Ru(dpbpy)(bpy)]) greatly enhanced the rate of CO_2 reduction to produce HCOOH and CO (entry 4). The neutral [Ru(dpbpy)] complex possessing phosphonate anchors generated the highest TON (equal to the HCOOH/[Ru(dpbpy)] ratio) among the photocatalysts evaluated in this work. A TON value of 104 was obtained after 16 h of irradiation, indicating greatly improved selectivity for HCOOH and CO as opposed to H_2, even though the [Ru(dpbpy)] had the most negative CO_2 reduction potential (-1.0 V) (entry 5). These results suggest that the photocatalytic activity might be dependent on the nature of the Ru-complex, such as its charge state, because in a control experiment under dark conditions, no products were generated (entry 6). The replacement of the phosphonate anchor with a carboxylate group decreased the CO_2 reduction activity, such that the TON for HCOOH decreased from 104 for [Ru(dpbpy)]/ZnS:Ni to 26 for [Ru(dcbpy)/ZnS:Ni] (entry 7). Assessing the effect of the charges of Ru-complexes with the same phosphonate anchors, the TON for HCOOH obtained from the neutral Ru-complex ([Ru(dpbpy)]/ZnS:Ni) was approximately three times that of the cationic [Ru(dpbpy)(bpy)]/ZnS:Ni. However, ZnS:Ni modified with the neutral Ru-complex possessing the most positive CO_2 reduction potential of -0.6 V *vs.* NHE ([Ru(pycbpy)]) showed a TON of only 23 for HCOOH generation (entry 8), similar to the values obtained from [Ru(dpbpy)(bpy)] and [Ru(dcbpy)]. This result is discussed in more detail further on.

Fig. 2 shows the progress of CO_2 reduction over a [Ru(dpbpy)]/ZnS:Ni hybrid photocatalyst under visible light irradiation. The catalyst maintained its photoactivity over an irradiation time span of 16 h. X-ray photoelectron spectroscopy (XPS) analyses of the photocatalyst before and after the reaction demonstrated that there was only minimal change in the oxidation state of S^{2-} ions and Ru ions in the ZnS:Ni after the photoreaction (Fig. S5). We also confirmed that the Ru-complex did not form Ru polymer [37] during photocatalytic reaction by measurement of UV–vis diffuse reflectance spectroscopy (Fig. S6). These results indicate that the hybrid photocatalyst was stable over this length of time. Assuming a monolayer modification of [Ru(dpbpy)] on the surface of ZnS:Ni, coverage of [Ru(dpbpy)] was estimated to be only 4%. It is wort noting that the slight amounts of Ru-complex molecular catalyst works efficiently as CO_2 reduction site on semiconductor surface.

Isotope tracer analyses using $^{13}CO_2$ also confirmed that the HCOOH was produced from CO_2 molecules dissolved in the solutions (Fig. 3). In the case of a photocatalytic reaction under $^{12}CO_2$, a clear peak at $m/z = 45$ due to formate ions containing ^{12}C is observed. In contrast, under a $^{13}CO_2$ atmosphere, the peak appears at $m/z = 46$ as the result of formate ions containing ^{13}C. Therefore, the carbon source for HCOOH was CO_2 molecules dissolved in the solution, suggesting that *n*-type ZnS:Ni is indeed viable as a component of hybrid photocatalysts

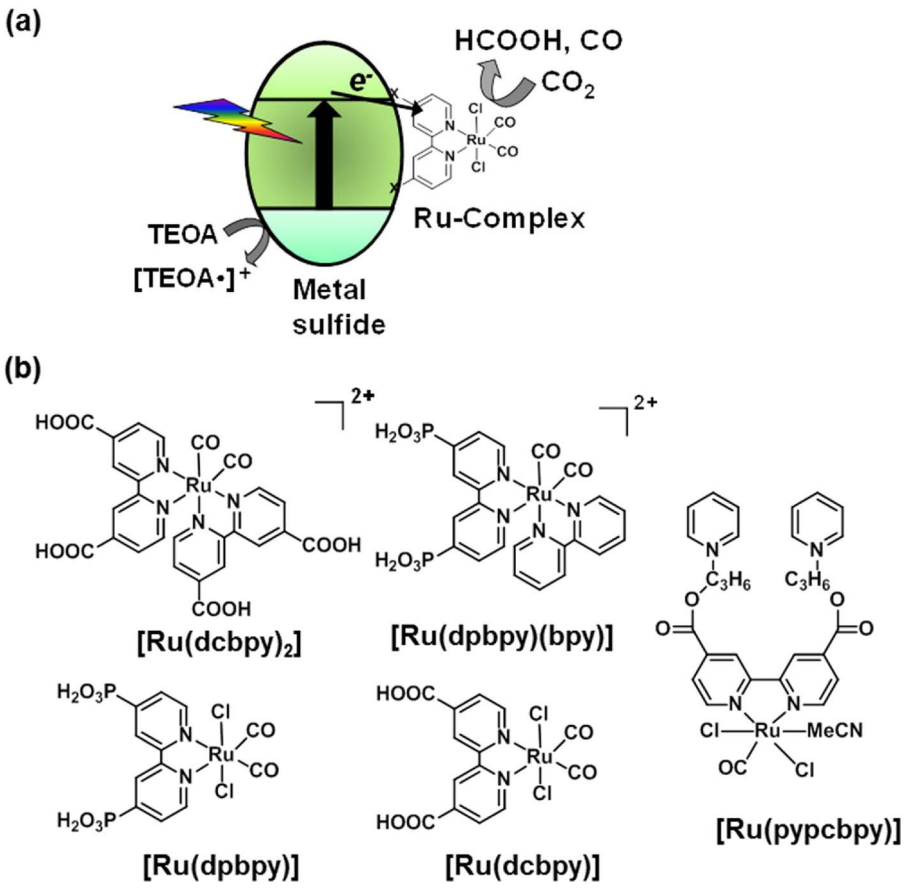

Fig. 1. (a) CO_2 reduction under visible light using a hybrid photocatalyst composed of a Ru-complex and metal sulfide semiconductor, and (b) the chemical structures of various Ru-complexes.

Table 1
Properties of various Ru-complexes.

Ru-complex	Chemical structure	Anchor	Charge	CO_2 reduction potential [V vs. NHE][a]
[Ru(dcbpy)$_2$]	[Ru(dcbpy)$_2$(CO)$_2$]$^{2+}$[b]	COOH	cationic	−0.8
[Ru(dpbpy)(bpy)]	[Ru(dpbpy)(bpy)(CO)$_2$]$^{2+}$[c,d]	PO_3H_2	cationic	−0.8
[Ru(dpbpy)]	Ru(dpbpy)(CO)$_2$Cl$_2$[c]	PO_3H_2	neutral	−1.0
[Ru(dcbpy)]	Ru(dcbpy)(CO)$_2$Cl$_2$[b]	COOH	neutral	N.D.[f]
[Ru(pypcbpy)]	Ru(pypcbpy)(CO)(MeCN)Cl$_2$[e]	–	neutral	−0.6

[a] CO_2 reduction potentials were obtained from cyclic voltammograms acquired in an acetonitrile (MeCN) solution under CO_2 (red) containing tetraethylammonium tetrafluoroborate (0.1 M) using a glassy carbon working electrode, a Pt counter electrode, and a I_2/I_3-(0.1 M) reference electrode. The threshold potentials giving large second peaks originating from secondary electron injection into CO_2 with Ru-complex were measured [5].

[b] dcbpy: 4,4′-dicarboxy-2,2′-bipyridine.

[c] dpbpy: 4,4′-diphosphonate-2,2′-bipyridine.

[d] bpy: 2,2′-bipyridine.

[e] Pypcbpy: 4,4′-di(1*H*-pyrrolyl-3-propyl carbonate)-2,2′- bipyridine.

[f] The reduction potential could not be determined because of low solubility in MeCN.

for CO_2 reduction under visible light irradiation.

As described in a previous report concerning Ru-complex/N-Ta_2O_5 hybrid photocatalysts, the enhanced CO_2 reduction activity can be explained primarily by two factors. The first is the direct connection between the semiconductor and the Ru-complex, and the second is the greater ΔG between the E_{CBM} of the semiconductor and the CO_2 reduction potential [typically almost equal to the lowest unoccupied molecular orbital (LUMO)] of the Ru-complex [5]. These points are important with regard to the enhancement of the electron transfer rate from the semiconductor to the Ru-complex. In this study, a neutral [Ru(dpbpy)] complex with phosphonate anchors was found to be the most

Table 2
Photocatalytic reduction of CO_2 in an organic solvent by Ru-complex/ZnS:Ni hybrid photocatalysts under visible light irradiation.[a]

Entry	Catalyst	Ru-complex content [wt %]	Light	Amounts of products [μmol]		
				H_2	CO (TON)[b]	HCOOH (TON)[b]
1	ZnS:Ni	0.00	On	0.31	0.00 (−)	0.00 (−)
2	[Ru(dpbpy)]	0.05[c]	On	0.00	0.00 (0)	0.00 (0)
3	[Ru(dcbpy)$_2$]/ZnS:Ni	0.07	On	0.62	0.01 (1)	0.04 (3)
4	[Ru(dpbpy)(bpy)]/ZnS:Ni	0.05	On	0.56	0.04 (7)	0.24 (35)
5	[Ru(dpbpy)]/ZnS:Ni	0.05	On	0.61	0.22 (32)	0.80 (104)
6	[Ru(dpbpy)]/ZnS:Ni	0.05	Off	0.00	0.00 (0)	0.00 (0)
7	[Ru(dcbpy)]/ZnS:Ni	0.05	On	0.39	0.04 (7)	0.20 (26)
8	[Ru(pypcbpy)]/ZnS:Ni	0.07	On	0.47	0.04 (5)	0.20 (23)

[a] Reaction conditions: catalyst (8 mg) in CO_2-saturated MeCN/TEOA (5/1, v/v) (4 mL) at ambient temperature. Suspensions were irradiated using a 500 W Xe lamp with filters to produce light in the range $390 < \lambda \leq 750$ nm over16 h. Product concentrations were determined by gas chromatography and ion-exchange chromatography. More than three runs were performed and the average values were calculated using them (within 4% error).

[b] Turnover numbers (TON) were calculated on the basis of the mass of metal complex used.

[c] Using the same amount of [Ru(dpbpy)] as for entry 5.

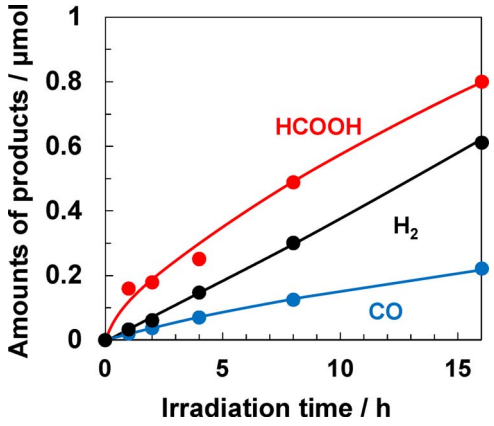

Fig. 2. CO_2 reduction in an organic solvent over a [Ru(dpbpy)]/ZnS:Ni hybrid powdered photocatalyst under visible light irradiation (λ > 390 nm). Conditions: catalyst (8 mg) in CO_2-saturated MeCN/TEOA (5/1, v/v) (4 mL) in a Pyrex glass test tube. More than three runs were performed and the average values were calculated using them (within 5% error).

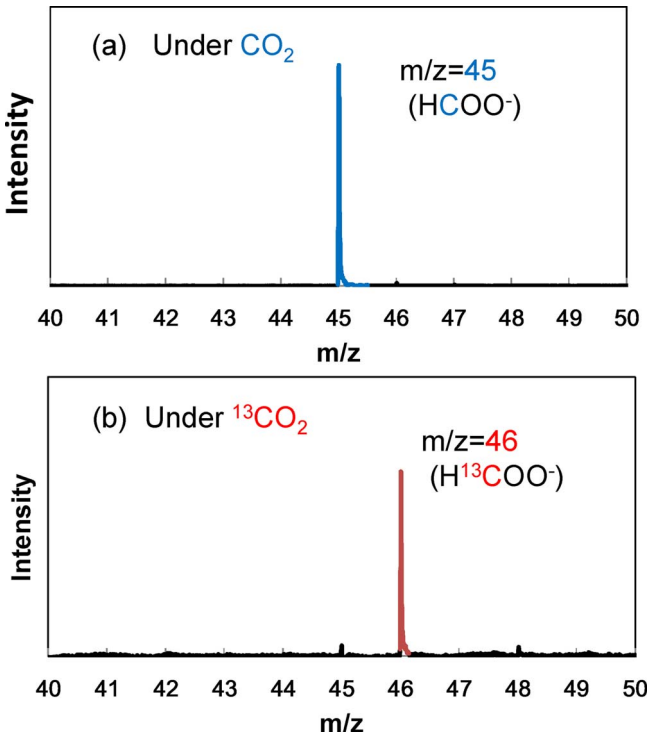

Fig. 3. ESI–MS spectra of the products ($HCOO^-$) in a liquid phase by photocatalytic reactions utilizing (a) $^{12}CO_2$ and (b) $^{13}CO_2$ over [Ru(dpbpy)]/ZnS:Ni under visible light irradiation (λ > 390 nm). Conditions: catalyst (10 mg) in $^{12}CO_2$ or $^{13}CO_2$-saturated MeCN/TEOA (5/1, v/v) (4 mL) in a Pyrex glass test tube, 6 h.

effective in combination with ZnS:Ni despite having the highest (that is, the most negative) CO_2 reduction potential of −1.0 V *vs.* NHE among the Ru-complexes, and so the smallest ΔG. Accordingly, the order of activity of these Ru-complex/ZnS:Ni hybrid photocatalysts must be explained by considering not only the driving force for electron transfer (ΔG) but also presumably the strength of bonding (in terms of non-adiabatic coupling and quantum coherence) between the Ru-complex and ZnS:Ni. Nonadiabatic molecular dynamics simulations for N-Ta_2O_5/Ru-complex materials have predicted that the anchoring groups determine the tilt angle of the complex on the semiconductor surface, which in turn is crucial for determining the electron transfer rate to the catalytic center [9].

In order to evaluate the effect of the Ni doping of ZnS, undoped ZnS

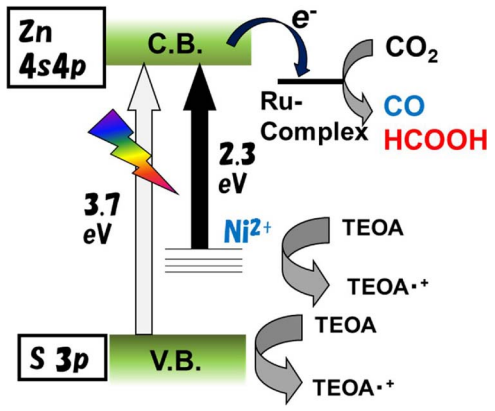

Fig. 4. Mechanism for the photoreduction of CO_2 by Ru-complex catalysts coupled with Ni-doped ZnS to produce hybrid photocatalysts.

and ZnS:Ni were assessed when modified with the [Ru(dpbpy)] catalyst. As shown in Figs. 4 and S7 , the Ni doping of ZnS creates a new energy level (due to the Ni 3d orbital) in the ZnS bandgap such that the energy gap is narrowed [21]. We initially irradiated the catalysts with wavelengths longer than 330 nm, which can activate both undoped and Ni-doped ZnSs [21]. As shown in Table 3, bare samples of undoped and Ni-doped ZnS evolved only H_2, and the amount of H_2 evolved over the ZnS:Ni was 4.4 times that produced by the undoped ZnS, due to the greater amount of photons absorbed by the doped material [21] (entries 9 and 11). In contrast, both undoped ZnS and ZnS:Ni, when modified with [Ru(dpbpy)], generated HCOOH and CO when exposed to wavelengths greater than 330 nm. Thus, both materials exhibited CO_2 photoreduction activity, suggesting electron transfer proceeded from the conduction bands of the photoexcited ZnS or ZnS:Ni to the [Ru(dpbpy)] as proposed in our previous study (Fig. 4) [5]. [Ru(dpbpy)]/ZnS generated HCOOH and CO because the E_{CBM} of ZnS formed by the Zn 4s4p orbitals is located at a sufficiently negative position (−1.3 V *vs.* NHE) to transfer electrons to [Ru(dpbpy)]. Under visible light irradiation, only [Ru(dpbpy)]/ZnS:Ni showed activity for photocatalytic CO_2 reduction. Therefore, it appears that the combination with [Ru(dpbpy)] imparts light-induced CO_2 reduction ability to both ZnS and ZnS:Ni, and so it should be possible to promote CO_2 reduction under visible light using many of the sulfide semiconductors reported to date.

3.2. Photocatalytic CO_2 reduction by ZnS-based solid solutions ($(GuGa)_{0.8}Zn_{0.4}S_2$ and $(AgIn)_{0.22}Zn_{1.56}S_2$) coupled with Ru-complexes

The above results demonstrate that ZnS:Ni materials with a sufficiently negative E_{CBM} are active for CO_2 reduction upon combining with Ru-complex catalysts, suggesting that sulfides should also be applicable to powdered hybrid systems for CO_2 reduction under visible light

Table 3
Photocatalytic reduction of CO_2 in an organic solvent by [Ru(dpbpy)]/ZnS and ZnS:Ni (0.2%) hybrid photocatalysts under UV and visible light irradiation.[a]

Entry	Metal sulfide	[Ru(dpbpy)] content (wt%)	Amounts of products [μmol]					
			λ > 330 nm			λ > 390 nm		
			H_2	CO	HCOOH	H_2	CO	HCOOH
9	ZnS	0.00	0.14	0.00	0.00	0.00	0.00	0.00
10	ZnS	0.14	0.08	0.02	0.04	0.00	0.00	0.00
11	ZnS:Ni	0.00	0.61	0.00	0.00	0.31	0.00	0.00
12	ZnS:Ni	0.05	0.73	0.26	0.89	0.61	0.22	0.80

[a] Reaction conditions: catalyst (8 mg) in CO_2-saturated MeCN/TEOA (5/1, v/v) (4 mL) at ambient temperature. Solutions ware irradiated using a 500 W Xe lamp with filters to produce light in the ranges λ > 330 nm or λ > 390 nm over 16 h. Product concentrations were determined by gas chromatography and ion-exchange chromatography.

Table 4
Photocatalytic reduction of CO_2 in an organic solvent by [Ru(dpbpy)]/$(CuGa)_{0.8}Zn_{0.4}S_2$ and $(AgIn)_{0.22}Zn_{1.56}S_2$ hybrid photocatalysts under visible light irradiation.[a]

Entry	Metal sulfide	Conduction type	Band gap (eV)	[Ru(dpbpy)] content (wt%)	Amounts of products [μmol]		
					H_2	CO (TON)[b]	HCOOH (TON)[b]
13	$(CuGa)_{0.8}Zn_{0.4}S_2$	*p*	2.2	0.00	4.54	0.00 (−)	0.12 (−)
14	$(CuGa)_{0.8}Zn_{0.4}S_2$	*p*	2.2	0.08	4.48	0.06 (5)	0.28 (12)
15	$(AgIn)_{0.22}Zn_{1.56}S_2$	*n*	2.4	0.00	0.66	0.02 (−)	0.24 (−)
16	$(AgIn)_{0.22}Zn_{1.56}S_2$	*n*	2.4	0.05	0.97	0.18 (15)	0.92 (126)

[a] Reaction conditions: catalyst (8 mg) in CO_2-saturated MeCN/TEOA (5/1, v/v) (4 mL) at ambient temperature. Solutions ware irradiated using a 500 W Xe lamp with filters to produce light in the range $390 < \lambda \leq 750$ nm over 16 h. Product concentrations were determined by gas chromatography and ion-exchange chromatography.
[b] Turnover numbers (TON) were calculated on the basis of the mass of metal complex used.

irradiation. To enhance the CO_2 photoreduction activity of such systems, we therefore prepared a hybrid photocatalyst composed of [Ru(dpbpy)] and Zn-based sulfide solid solution semiconductors, $(CuGa)_{0.8}Zn_{0.4}S_2$ (*p*-type) [24] and $(AgIn)_{0.22}Zn_{1.56}S_2$ (*n*-type) [26,27], with band gaps of 2.2 and 2.4 eV, respectively (Fig. S7). Table 4 summarizes the results of photocatalytic CO_2 reduction reactions under visible light irradiation. $(CuGa)_{0.8}Zn_{0.4}S_2$ and $(AgIn)_{0.22}Zn_{1.56}S_2$ possessed CO_2 photoreduction activity and produced HCOOH even when not modified with [Ru(dpbpy)]. In contrast, modification with [Ru(dpbpy)] induced CO formation, which suggested [Ru(dpbpy)] acted as CO_2 reduction catalyst. Accordingly, HCOOH formation rate greatly improved by the linkage with [Ru(dpbpy)]. It is noteworthy that H_2 was the major product over the [Ru(dpbpy)]/$(CuGa)_{0.8}Zn_{0.4}S_2$. In contrast, the [Ru(dpbpy)]/$(AgIn)_{0.22}Zn_{1.56}S_2$ exhibited the highest photocatalytic activity for the reaction of CO_2 to HCOOH among the hybrid photocatalysts assessed in this work. The TON for HCOOH after 16 h irradiation obtained from this system was 126, a value that exceeds the TON observed for ([Ru(dpbpy)]/ZnS:Ni). $(AgIn)_xZn_{2(1-x)}S_2$ is well known to be a unique luminescent material [38,39] and it is thought that the long photoexcited state lifetime of this semiconductor enhanced the efficiency of the electron transfer from the semiconductor to the Ru-complex, resulting in the observed excellent CO_2 reduction photoactivity. In the case of the [Ru-bpy]/N-Ta_2O_5 powdered system, the anchoring groups in the Ru-complex that link to the semiconductor surfaces also have a significant effect in terms of generating higher CO_2 photoreduction rates and TONs. This has been demonstrated by both experimental work and nonadiabatic molecular dynamics simulations [5,6,8,9]. Hence, the electronic structure in the vicinity of the semiconductor-complex interface could also explain the high TON observed in the present work. The carbon source for the formic acid evolved in the reaction over [Ru(dpbpy)]/$(AgIn)_{0.22}Zn_{1.56}S_2$ was again confirmed to be CO_2 based on $^{13}CO_2$ analyses (Fig. S8).

Here, we discuss CO_2 photoreduction over solid solution sulfide/Ru-complex systems. The conduction bands of $(CuGa)_{0.8}Zn_{0.4}S_2$ and $(AgIn)_{0.22}Zn_{1.56}S_2$ are primarily composed of Zn4s4p + Ga 4s4p [24] and Zn4s4p + In 5s5p orbitals [26], respectively. The conduction band formed by Zn 4s4p orbitals is located at a position more negative than that of the Ga 4s4p and In 5s5p orbitals [24,26]. Therefore, the E_{CBM} levels of these materials are in the order of: ZnS:Ni < ($CuGa)_{0.8}Zn_{0.4}S_2$ < $(AgIn)_{0.22}Zn_{1.56}S_2$. On a thermodynamic basis, ZnS:Ni is thus considered to possess the best E_{CBM} for electron transfer to the LUMO of the Ru-complex among these sulfide semiconductors. However, order of CO_2 reduction rates were of ($CuGa)_{0.8}Zn_{0.4}S_2$ < ZnS:Ni < $(AgIn)_{0.22}Zn_{1.56}S_2$. In our previous study using a metal oxide semiconductor [5], it was proposed that *p*-type N-Ta_2O_5 is favorable for the construction of hybrid systems. In contrast, the present work demonstrates that *n*-type semiconductors such as ZnS:Ni and $(AgIn)_{0.22}Zn_{1.56}S_2$ are effective. These results strongly indicate that the CO_2 photoreduction efficiency of the hybrid photocatalyst is not determined only by the ΔG associated with the E_{CBM} and the conduction type. Hence, other critical factors, such as the nature of the semiconductor (the extent of light absorption, defects and crystallinity among others) and the linkage (coupling, quantum coherence, *etc*.) between the Ru-complex and the semiconductor are suggested. It is widely accepted that HCOOH/CO selectivity at the metal complexes is dependent on electronic state of central metal governed by ligand species and solvent, although details of the reaction mechanism have not yet been clarified [40]. The HCOOH/CO ratios generated at the Ru-complex over these sulfide semiconductors linked with [Ru(dpbpy)] in the aprotic solvent were 3.6, 2.7, 4.3 for ZnS:Ni, $(CuGa)_{0.8}Zn_{0.4}S_2$, and $(AgIn)_{0.22}Zn_{1.56}S_2$, respectively. This reproducible fact suggested possible difference in electronic structure of the [Ru(dpbpy)] linked with the semiconductors, which could modify a balance of reaction pathway to form CO and HCOOH involving reaction with electrons and protons [40].

CO_2 reduction to HCOOH over [Ru(bpbpy)]/$(AgIn)_{0.22}Zn_{1.56}S_2$ was found to proceed for 8 h under visible light irradiation (Fig. S9), after which the reaction rate gradually decreased. XPS analysis following 16 h of the photocatalytic reaction showed that the evident deactivation was not due to deterioration of the semiconductor, such as via changes in the chemical states of the S or Ag (Fig. S7), but rather because of the elimination of approximately 80% of the Ru-complex from the $(AgIn)_{0.22}Zn_{1.56}S_2$ surface, judging from changes in the Ru/Zn and Ru/S atomic ratios (Table S1). The stability of this material could potentially be improved by obtaining a more stable interface between the Ru-complex and $(AgIn)_{0.22}Zn_{1.56}S_2$.

N-Ta_2O_5 and C_3N_4 are recognized as relatively inert semiconductors for both H_2 generation and CO_2 reduction [5,13,35], and enhancement of CO_2 reduction selectivity has clearly been observed by the linkage with metal-complex catalysts, in which C_3N_4-based system showed a very high turnover number of greater than 1000 [5,13]. In addition, it was reported that solvents and sacrificial reagents largely affect photocatalytic activity of C_3N_4-based hybrid catalyst such as efficiency and selectivity [37], because of the difference in ability of their reaction parameters including electron transfer rate, acidity/basicity, and CO_2 concentration, *etc*. While, Reisner group demonstrated that selectivity for CO generation over CdS, a relatively active photocatalyst for CO_2 photoreduction [41], was highly enhanced by an appropriate conjugation with a metal-complex [30]. These results suggest that further improvement of various sulfide-based semiconductor/metal-complex systems is expected by means of improving catalyst coverage, electron transfer associated with electronic structure by solvents and conjugation, *etc*.

4. Conclusions

This work demonstrated powdered photocatalysts for CO_2 reduction, employing various Zn-based metal sulfide semiconductors hybridized with Ru-complex catalysts under visible light irradiation in the presence of electron donor. The photocatalytic activities were found to be largely dependent on the basic characteristics of the Ru-complex and the metal sulfide, such as polarity and the photoexcited state lifetime. Combinations of a neutral Ru-complex containing phosphonate anchors and *n*-type $(AgIn)_{0.22}Zn_{1.56}S_2$ or Ni-doped ZnS showed highly enhanced

TON values for HCOOH. Metal sulfides should therefore be applicable to the fabrication of metal complex/semiconductor hybrid systems for CO_2 reduction. The data show that the degree of CO_2 reduction activity is not explained by the strength of the interaction or by the energy difference between the semiconductor and Ru-complex, as was proposed in a previous study using metal oxide semiconductors. Our results also suggest that further study could potentially improve the activity of these hybrid photocatalysts and it is expected that metal sulfides will be applicable to future powdered Z-scheme systems utilizing water as an electron donor and proton source.

Acknowledgements

T.M.S., S.S. and T.M. were partially supported by the Advanced Catalytic Transformation Program for Carbon Utilization (ACT-C) of the Japan Science and Technology Agency (JST). The authors thank Mr. Akira Ikeda, Mr. Tomotaka Yamamoto, Mr. Ikko Honma, Mr. Takeshi Miyazono, Mr. Shunya Yoshino and Mr. Ikoma Narita for experimental assistance. The authors also thank Ms. Naoko Takahashi and Mr. Kousuke Kitazumi (XPS analyses) and Dr. Soichi Shirai (quantum chemical calculation).

Appendix A. Supplementary data

Supplementary data associated with this article can be found, in the online version, at http://dx.doi.org/10.1016/j.apcatb.2017.10.053.

References

[1] F.F. Abdi, L.H. Han, A.H.M. Smets, M. Zeman, B. Dam, R. van de Krol, Nat. Commun. 4 (2013) 2195.
[2] K.J.P. Schouten, Z.S. Qin, E.P. Gallent, M.T.M. Koper, J. Am. Chem. Soc. 134 (2012) 9864.
[3] B.A. Pinaud, J.D. Benck, L.C. Seitz, A.J. Formanm, Z. Chen, T.G. Deutsch, B.D. James, K.N. Baum, G.N. Baum, S. Ardo, H. Wang, E. Miller, T.F. Jaramillo, Energy Environ. Sci. 6 (2013) 1983.
[4] T. Morikawa, S. Saeki, T. Suzuki, T. Kajino, T. Motohiro, Appl. Phys. Lett. 96 (2010) 142111.
[5] S. Sato, T. Morikawa, S. Saeki, T. Kajino, T. Motohiro, Angew. Chem. Int. Ed. 49 (2010) 5101.
[6] T.M. Suzuki, H. Tanaka, T. Morikawa, M. Iwaki, S. Sato, S. Saeki, M. Inoue, T. Kajino, T. Motohiro, Chem. Commun. 47 (2011) 8673.
[7] T.M. Suzuki, T. Nakamura, S. Saeki, Y. Matsuoka, H. Tanaka, K. Yano, T. Kajino, T. Morikawa, J. Mater. Chem. 22 (2012) 24584.
[8] A.V. Akimov, R. Jinnouchi, S. Shirai, R. Asahi, O.V. Prezhdo, J. Phys. Chem. B 119 (2015) 7186.
[9] A.V. Akimov, R. Asahi, R. Jinnouchi, O.V. Prezhdo, J. Am. Chem. Soc. 137 (2015) 11517.
[10] K. Yamanaka, S. Sato, M. Iwaki, T. Kajino, T. Morikawa, J. Phys. Chem. C 115 (2011) 18348.
[11] K. Sekizawa, K. Maeda, K. Domen, K. Koike, O. Ishitani, J. Am. Chem. Soc. 135 (2013) 4596.
[12] A. Nakada, T. Nakashima, K. Sekizawa, K. Maeda, O. Ishitani, Chem. Sci. 7 (2016) 4364.
[13] R. Kuriki, K. Sekizawa, O. Oshitani, K. Maeda, Angew. Chem. Int. Ed. 14 (2015) 2406.
[14] R. Kuriki, H. Matsunaga, T. Nakashima, K. Wada, A. Yamakata, O. Ishitani, K. Maeda, J. Am. Chem. Soc. 138 (2016) 5159.
[15] G. Neri, J.J. Walsh, C. Wilson, A. Reynal, J.Y.C. Lim, X. Li, A.J.P. White, N.J. Long, J.R. Durrant, A.J. Cowan, Phys. Chem. Chem. Phys. 17 (2015) 1562.
[16] A. Kudo, Y. Miseki, Chem. Soc. Rev. 38 (2009) 253.
[17] M. Matsumura, Y. Saho, H. Tusbomura, J. Phys. Chem. 87 (1983) 3807.
[18] J.F. Reber, M. Rusek, J. Phys. Chem. 90 (1986) 824.
[19] N. Kakuta, K.H. Park, M.F. Finlayson, A. Ueno, A.J. Bard, A. Campion, M.A. Fox, S.E. Webber, J.M. White, J. Phys. Chem. 89 (1985) 732.
[20] J.F. Reber, K. Meier, J. Phys. Chem. 88 (1984) 5903.
[21] A. Kudo, M. Sekizawa, Chem. Commun. (2000) 1371.
[22] A. Kudo, M. Sekizawa, Catal. Lett. 58 (1999) 241.
[23] I. Tsuji, A. Kudo, J. Photochem. Photobiol. A 156 (2003) 249.
[24] T. Kato, T. Hakari, S. Ikeda, Q. Jia, A. Iwase, A. Kudo, J. Phys. Chem. Lett. 6 (2015) 1042.
[25] A. Kudo, I. Tsuji, H. Kato, Chem. Commun. 17 (2002) 1958.
[26] I. Tsuji, H. Kato, H. Kobayashi, A. Kudo, J. Am. Chem. Soc. 126 (2004) 13406.
[27] I. Tsuji, H. Kato, A. Kudo, Chem. Mater. 18 (2006) 1969.
[28] I. Tsuji, H. Kato, H. Kobayashi, A. Kudo, J. Phys. Chem. B 109 (2005) 7323.
[29] T. Takayama, K. Sato, T. Fujimura, Y. Kojima, A. Iwase, A. Kudo, Faraday Discuss. 198 (2017) 397.
[30] M.F. Kuehnel, K.L. Orchard, K.E. Dalle, E. Reisner, J. Am. Chem. Soc. 139 (2017) 7217.
[31] T. Arai, S. Tajima, S. Sato, K. Uemura, T. Morikawa, T. Kajino, Chem. Commun. 47 (2011) 12664.
[32] P.A. Anderson, G.B. Deacon, K.H. Haarmann, F.R. Keene, T.J. Meyer, D.A. Reitsma, B.W. Skelton, G.F. Strouse, N.C. Thomas, J.A. Treadway, A.H. White, Inorg. Chem. 34 (1995) 6145.
[33] T.M. Suzuki, A. Iwase, H. Tanaka, S. Sato, A. Kudo, T. Morikawa, J. Mater Chem. A 3 (2015) 13283.
[34] H. Tian, ChemSusChem 8 (2015) 3746.
[35] Y. Tomita, S. Teruya, O. Koga, Y. Hori, J. Electrochem. Soc. 147 (2000) 4164.
[36] T.M. Suzuki, S. Saeki, K. Sekizawa, K. Kitazumi, N. Takahashi, T. Morikawa, Appl. Catal. B 202 (2017) 597.
[37] R. Kuriki, O. Ishitani, K. Maeda, ACS Appl. Mater. Interfaces 8 (2016) 6011.
[38] H. Nakamura, W. Kato, M. Uehara, K. Nose, T. Omara, S.O.Y. Matuo, M. Miyazaki, H. Maeda, Chem. Mater. 18 (2006) 3330.
[39] T. Torimoto, T. Adachi, K. Okazaki, M. Sakuraoka, T. Shibayama, B. Ohtani, A. Kudo, S. Kuwabata, J. Am. Chem. Soc. 129 (2007) 12388.
[40] A.J. Morris, G.J. Meyer, E. Fujita, Acc. Chem. Res. 42 (2009) 1983.
[41] H. Fujiwara, H. Hosokawa, K. Murakoshi, Y. Wada, S. Yanagida, J. Phys. Chem. B 101 (1997) 8270.